View Online / Journal Homepage
Dynamic Article Links

Integrative Biology

Cite this: DOI: 10.1039/c1ib00039j

www.rsc.org/ibiology

TECHNICAL INNOVATION

Protein–DNA interactions in high speed AFM: single molecule diffusion analysis of human RAD54†

Humberto Sanchez,*[a] Yuki Suzuki,[b] Masatoshi Yokokawa,[b] Kunio Takeyasu[b] and Claire Wyman[ac]

Received 29th April 2011, Accepted 18th September 2011
DOI: 10.1039/c1ib00039j

High-speed AFM (atomic force microscopy also called scanning force microscopy) provides nanometre spatial resolution and sub-second temporal resolution images of individual molecules. We exploit these features to study diffusion and motor activity of the RAD54 DNA repair factor. Human RAD54 functions at critical steps in recombinational-DNA repair. It is a member of the Swi2/Snf2 family of chromatin remodelers that translocate on DNA using ATP hydrolysis. A detailed single molecular description of DNA–protein interactions shows intermediate states and distribution of variable states, usually hidden by ensemble averaging. We measured the motion of individual proteins using single-particle tracking and observed that random walks were affected by imaging-buffer composition. Non-Brownian diffusion events were characterized in the presence and in the absence of nucleotide cofactors. Double-stranded DNA immobilized on the surface functioned as a trap reducing Brownian motion. Distinct short range slides and hops on DNA were visualized by high-speed AFM. These short-range interactions were usually inaccessible by other methods based on optical resolution. RAD54 monomers displayed a diffusive behavior unrelated to the motor activity.

Introduction

Diffusive movements of proteins have been extensively studied by biochemical means[1–3] and fluorescence microscopy.[4–7] Translocation of motor proteins on DNA facilitates finding a specific site or sequence location. In order to determine if a protein slides, hops or jumps between DNA sites[8] short-range interaction between DNA need to be analyzed. Globular proteins typically have a diameter between 2 and 10 nm, and intermolecular motions occur in a time scale ranging from nanoseconds to milliseconds.[9]

Measurements of association rates of protein with specific DNA sites or locations lead to the conclusion that protein diffusion can be 'facilitated', in some cases being almost two order of magnitudes faster than expected by free diffusion.[1] This diffusion limit depends on the neutralization of surface charge by solvent counter-ions.[10] Protein diffusion along DNA can be directly observed by single molecule microscopy of fluorescently label proteins. Despite the high temporal resolution achievable by this method using the current

[a] *Department of Cell Biology and Genetics, Cancer Genomics Center, Erasmus MC, PO Box 2040, 3000 CA Rotterdam, The Netherlands. E-mail: h.sanchezgonzalez@erasmusmc.nl; Fax: +31 (0)10 704 4743; Tel: +31 (0)10 704 3158*
[b] *Laboratory of Plasma Membrane and Nuclear Signaling, Graduate School of Biostudies, Kyoto University, Yoshida-Konoe-cho, Sakyo-ku, Kyoto 606-8501, Japan*
[c] *Department of Radiation Oncology, Erasmus MC, PO Box 2040, 3000 CA Rotterdam, The Netherlands*

† Electronic supplementary information (ESI) available: Supplementary software, Fig. S1–S4 and Movies 1–4. See DOI: 10.1039/c1ib00039j

Insight, innovation, integration

Dynamic optical microscopy has shown protein/DNA interaction with high temporal resolution. However, nanometre-spatial resolution is still technically difficult. Proteins find specific DNA sites or sequence location by sliding along the DNA strand or hopping between DNA sites. Sliding and hopping events require high spatial and high temporal resolution in order to be fully analyzed. Here, we introduce High-speed Atomic Force Microscopy as a valuable technique for the study of protein/DNA dynamics at the single molecule level. We validate the technique by using the human DNA repair factor RAD54 and provide software tools based on single-particle tracking (SPT) for the analysis of high-speed AFM movies. This offers new ways of addressing highly dynamic processes of proteins interacting with and doing work on DNA.

EMCCD cameras (500 frames per s), nanometre-spatial resolution is still technically challenging in dynamic optical microscopy. Spatial information from collected photons can be maximized and images super-resolved only if a sufficient number of events are acquired.[11] In practice, individual image frames are compiled by integrating hundred milliseconds of continuous exposure, in experimentally favourable cases.[12] So, the information recovered is the sum of all the events occurring in the acquisition period. Individual sliding or hopping events would not be resolved in this time window. Sliding or hopping of proteins has been deduced mainly by looking at changes in the diffusion constant after varying salt concentration.[5,13]

Atomic force microscopy (AFM) is a valuable technique for studying DNA–protein interactions.[14–17] Imaging in buffer enables the visualization of biochemically active complexes[18–20] and has been used for studying protein diffusion on a surface.[21,22]

Nanometre spatial resolution is standardly achieved using sharp tips with an end radius smaller than 10 nm. Relatively large and semi-flexible polymers like DNA are visible without stretching. However the temporal resolution of conventional AFM (tens of seconds per frame) is several orders of magnitude lower than the required for matching the speed of protein diffusion. High-speed AFM based on the use of small cantilevers and fast feedback control[23,24] allows scanning biological samples in buffer up to 30 frames per second. This method has been employed recently to show the "walking" behaviour of Myosin V on actin filaments.[25] High-speed AFM has also been used to study dynamic protein–DNA complexes: restriction enzymes moving and cutting DNA[26–28] and nucleosomes sliding and dissociating.[29] These previous works show that the Brownian motion of proteins over the mica surface used for imaging is not affected by the speed of scanning. However the effect of different imaging buffer conditions on the motion of proteins on the surface has not been specifically tested.

Single-particle tracking (SPT) was developed for diffusion analysis of proteins and lipids in cellular membranes.[30–36] Diffusion properties of fluorescently labeled proteins and nucleic acids in the cell nucleus[37–39] and viral particles in prokariots[40] and eukariots[41] have also been studied by SPT. The trajectory over time is recorded and the mean-square displacement used to characterize the movement of labeled particles. Here we used SPT for analyzing the diffusion properties of RAD54 directly visualized by high-speed AFM.

Human RAD54 is a protein involved in DNA repair by homologous recombination.[42–44] This process mediates the exchange of genetic information between homologous DNA molecules and requires the concerted action of several proteins. RAD54 interacts in a sequence-independent manner with DNA and is a motor protein that can move by tracking along the helix.[45] It has a double-stranded DNA-dependent ATPase activity.[46] Previous AFM imaging suggests that plectonemic supercoils are created by RAD54 protein oligomers anchored at some point on DNA and moving along the helix at another site.[47] This mechanism of action implies the concerted occurrence of non-specific interactions followed by a movement of the protein. Thus RAD54 is a good candidate protein to exhibit a variety of interactions with DNA, encompassing relevant time and length scales, including non-specific short-range and ATP driven long-range movements. In order to analyze both non-specific interaction and motor activity along DNA, we applied high-speed AFM to achieve the required spatial and temporal resolution. We directly visualized the sliding and hopping of RAD54 monomers. Moreover, we revealed by SPT analysis that monomeric RAD54 shows ATP-independent dynamics.

Results

Analysis of diffusion variations due to protein–surface interactions and composition of the imaging buffer

Imaging of protein dynamics on DNA molecules by AFM strongly depends on buffer composition. DNA molecules must be attached to the surface and at the same time be partially free to avoid steric hindrance to protein interaction. Bivalent cations, like magnesium, are used to bridge DNA molecules to the negatively charged mica surface. Supercoiled plasmid DNA and human RAD54 protein were deposited in conditions favouring the partial attachment of the DNA to mica using 2 mM $MgCl_2$. In these conditions variations in protein mobility were studied by SPT from high-speed AFM movies. Several mathematical approaches exist to analyze particle motion. Popular methods are based on estimation of diffusion coefficients after averaging the particle square displacements as a function of the time lag.[30,31,48,49] This method allows a straightforward discrimination between Brownian and anomalous diffusion. However, because of the averaging procedure, information about individual steps is lost. On the contrary, analysis of displacement-steps distribution[35,50–52] could show subtle variations between different conditions.

We first analyzed how nucleotides influence protein mobility (by measuring the hopping length on mica) in the AFM fluid cell before determining the effect of nucleotide on interactions with DNA. ATP is a nucleotide cofactor essential for RAD54 functions. At pH 8, ATP molecules are mainly (90%)[53] as $ATPMg^{2-}$ potentially changing mica-surface charge. Different nucleotide composition results in different movement of the proteins as observed by high-speed AFM. To quantitatively assess this difference we studied single proteins that did not interact with DNA. We measured the protein displacement between consecutive frames over time. Distributions of all measured steps in each conditions coming from different protein trajectories were pooled together. Using a normalized cumulative distribution of lengths (Fig. 1) we determined that the probability that a protein makes a displacement of at least 10 nm (smaller lengths were below the achievable resolution with the scanning tips employed) was lower in the absence of nucleotide than in the presence of 5 mM ATP (P_{10} = 0.056 and P_{10} = 0.088, respectively). Buffer without nucleotide supplemented with 5 mM $MgCl_2$ resulted in equivalent probability (P_{10} = 0.04) as buffer without ATP. Whereas the probability was almost one order of magnitude higher in buffer with AMP-PNP (P_{10} = 0.30) (data not shown). These results indicated that the effect of protein diffusion on the mica surface was nucleotide dependent but independent of ATP hydrolysis.

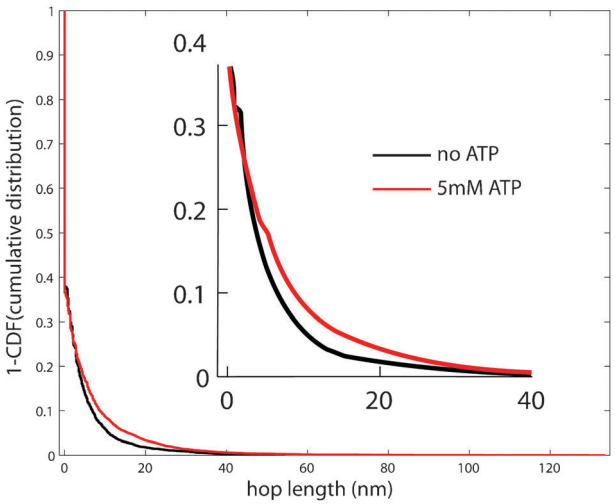

Fig. 1 Length distributions of movements made by individual RAD54 protein on mica with or without ATP. The cumulative distribution of hop lengths (nm) was normalized by the total number of movements. Black line = no ATP (n = 7768 steps); red line = 5 mM ATP (n = 10 454 steps).

Single particle tracking of individual proteins is possible with high-speed AFM. Isolated displacements can be analyzed in order to test the effect of buffer composition on the diffusive characteristics of proteins on the surface (Fig. 2). Trajectory of individual proteins was directly visualized and measured. Frequency of pauses (*fpauses*), diffusion coefficient (D) and α factor were calculated for each protein. This latter parameter shows the deviation of the displacement from an ideal 'normal' diffusive movement. Brownian movements display a linear growth of the mean square displacement (MSD) with respect to time (Δt), so that the scaling factor α equals one. In two-dimensions, this relation is described by:

$$\langle r^2 \rangle = \mathrm{MSD}(\Delta t) = 4D\Delta t^{\alpha} \quad (1)$$

Different values of α result from anomalous diffusion and can be found by a linear fit to:

$$\log(\mathrm{MSD}(\Delta t)) = \alpha \log(\Delta t) + \log(4D) \quad (2)$$

Distribution analyses of single displacements show that the absence of nucleotide in the imaging buffer favours the random movement of proteins (Fig. 3). Continuity of the

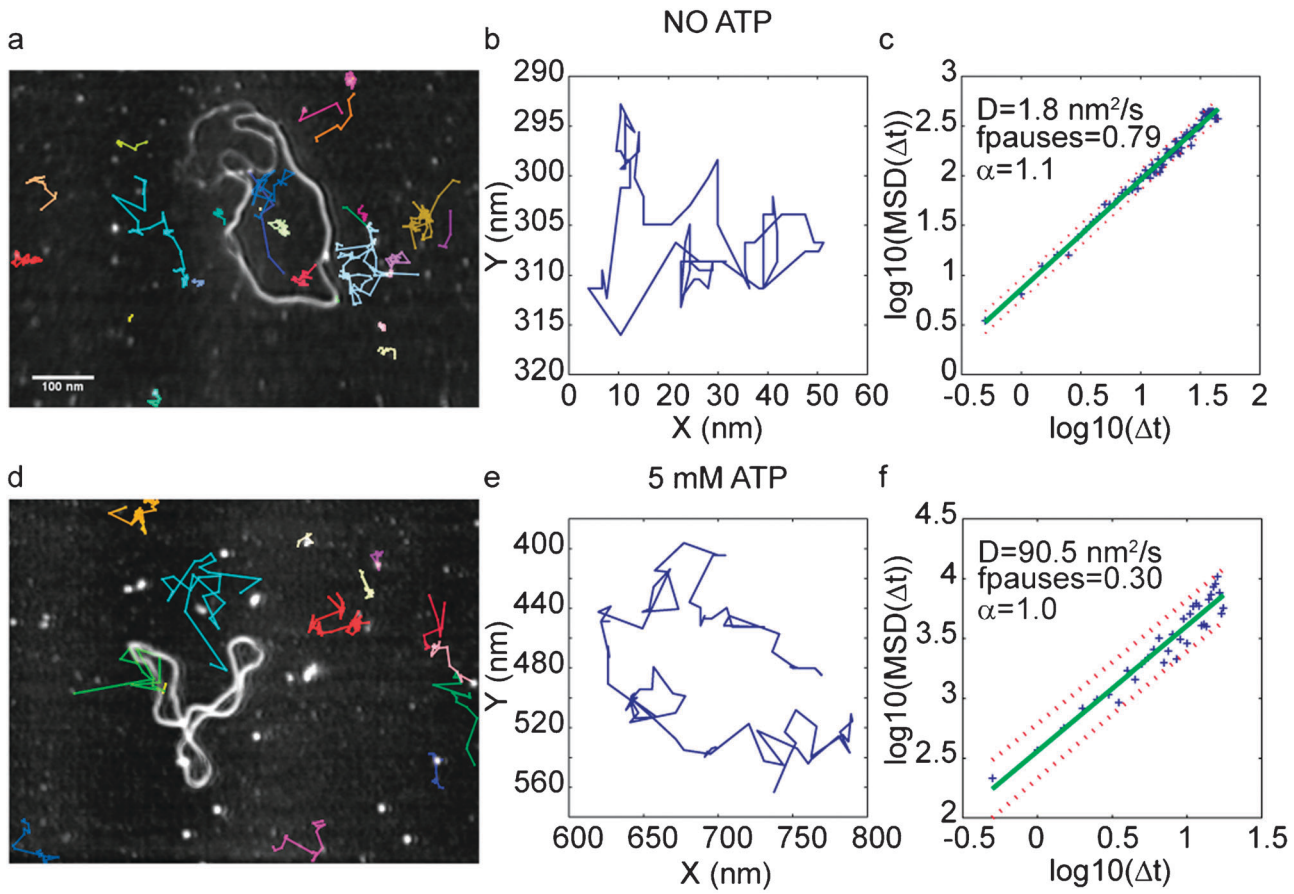

Fig. 2 Single protein diffusion analysis by high-speed AFM. (a, d) Sample trajectories used for analysis were traced in colors and overlaid with a picture representing the median intensity value for all the frames from the AFM movies. Original scan area, 800 × 600 nm^2. Brighter intensity pixels indicate stronger interaction with the surface, while blurry or diffuse pixels indicate a weak interaction. Representative displacements are shown to exemplify the analysis performed with all the particles. The coordinates in x and y from the particle position in consecutive frames were calculated, linked and plotted in (b) and (e) to show the shape of the displacement. The Log (MSD (Δt)) *versus* the log (Δt) plots (c), (f) were used for the calculation of the α factor and the diffusion coefficient (D). Green lines = linear fit of the data. Red discontinuous lines = prediction bounds (95% confidence).

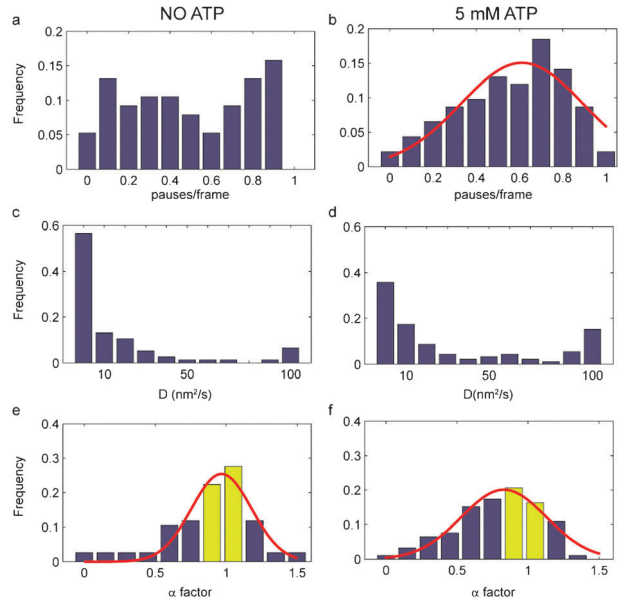

Fig. 3 Population analysis of single protein diffusion. Histograms showing the distribution of pauses/frames in the absence of nucleotide (a) or with 5 mM ATP (b); red line in (b) is the 'normal' fitting of the data; (c, d) distribution of diffusion coefficients of individual proteins in the absence of nucleotide or with 5 mM ATP, respectively; (e, f) distribution of α factor in the absence of nucleotide or with 5 mM ATP, respectively. Bins in yellow = Brownian diffusion, 50% in (e) and 37% in (f).

trajectories (*fpauses*) varies from stalls to a continuous movement without pauses (Fig. 3a). The diffusion coefficient was lower than 10 $nm^2\ s^{-1}$ for 56% of the proteins (Fig. 3c). Moreover, 50% of the trajectories showed a linear increase of the MSD with respect to time ($0.75 < \alpha < 1.05$, Fig. 3e). In contrast, the presence of 5 mM ATP in the imaging buffer resulted in a biased continuity centered at 0.61 pauses per frame ($r^2 = 0.8$) (Fig. 3b). The number of molecules irreversibly bound to the surface also increased with the presence of nucleotide (35 *versus* 53 in the example shown in Fig. 2). With ATP in solution, 20% of the molecules analyzed diffused faster than 80 $nm^2\ s^{-1}$ (Fig. 3d). There were fewer particles (37%) moving with a clear Brownian behaviour (Fig. 3f). Additionally, 51% of the particles had an α factor between 0 and 0.75 (anomalous sub-diffusion), and 12% of the particles had an α factor between 1.05 and 1.5 (anomalous super-diffusion) (Fig. S1, ESI†).

We determined the multimeric state of the protein by volume analysis as described before.[14,26] This showed a homogeneous distribution that fit well ($r^2 = 0.99$) with a Gaussian centered at 101.2 ± 30.1 (SD) nm^3, corresponding to monomers of 84 kDa as the diffusive particles analyzed (Fig. S2, ESI†). The diffusion constant for a globular protein of 84 kDa in water at 30 °C is 96×10^6 $nm^2\ s^{-1}$ (from the Stokes–Einstein equation), several orders of magnitude higher than the experimental results. The observed reduced diffusion constant is likely due to the interaction with the surface. Analysis of surface interactions is needed in order to understand the diffusive behavior in a more complex situation including diffusion along DNA.

Single molecule observation of constrained mobility due to a physical barrier: DNA corrals reduce RAD54 mobility

In order to determine the influence of DNA on protein diffusion, DNA was immobilized in the presence of RAD54. The influence of crowded environments on protein diffusion has been studied in experiments with optical resolution (using fluorescently label proteins) and by computer simulations based on assumptions.[54–56]

We could address directly and with high spatial resolution the relative movement of protein and DNA and their mutual influence. By reducing the dimensionality of the system (from 3D to 2D) a simplified model allows detailed analysis of protein behavior. Deposition of circular DNA and proteins together resulted in some proteins within the circles. The displacements of proteins included in DNA-corrals were selected for analysis (Fig. 4 and Movies 1 and 2, ESI†). Displacements were measured as described above and represented as an overlay on the averaged image (pixel intensity correlates with duration of surface interaction) (Fig. 4a and d). Diffusion constant and α factor of the individual proteins were calculated after plotting Log (MSD (Δt)) *versus* log (Δt) (Fig. 4c and f). Proteins moving inside smaller corrals (Fig. 4d) are more constrained than when the area delimited by the DNA corral was larger (Fig. 4a). The apparent diffusion coefficient for proteins in small-corralled areas was consequently lower (9.8 $nm^2\ s^{-1}$ *versus* 112.4 $nm^2\ s^{-1}$), as was the α factor (from 0.92 to 0.69) showing a variation from random walks. Apparently DNA was not a physical barrier because proteins were observed jumping from one side of the corral to the other (Fig. 4a; Movie 1, ESI†). We conclude that the anionic nature of DNA likely constrained protein movement by acting as a high local-density charge-matrix. We have shown that DNA corrals reduce the mobility of individual proteins, validating the analysis method.

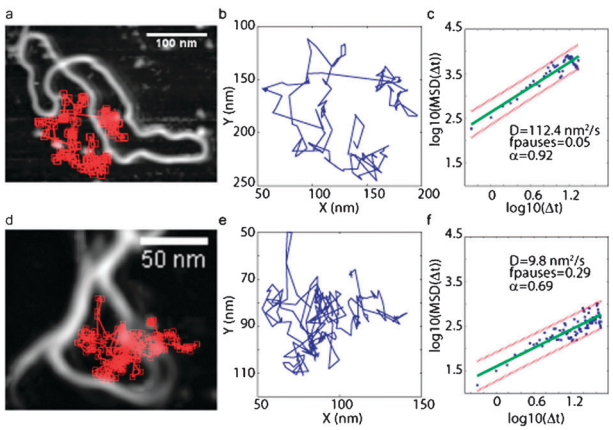

Fig. 4 Local concentration of DNA affects the free diffusion of the protein. (a, d) Overlay of protein displacement and a picture representing the median intensity value for all the frames from Movies 1 and 2 (ESI†), respectively (cropped images; original scan sizes 800 × 600 nm). (b, e) Scatter plot of *x* and *y* coordinates from (a) and (d), respectively. (c, d) Plot of the Log (MSD (Δt)) of the individual proteins *versus* log (Δt). Green lines = linear fit of the data. Red discontinuous lines = prediction bounds (95% confidence).

Direct observation of protein hopping and sliding on DNA by high-speed AFM

The ability of proteins to find specific locations on DNA has been recognized as "facilitated" by non-specific interactions. To observe distinct protein dynamic behaviors like, hopping and sliding, requiring high spatial and high temporal resolution we used high speed AFM. Identification of sliding, hopping or jumping of proteins between DNA sites depends on the spatial and temporal resolution of the technique used. We analyzed the movement of proteins that interact with DNA at the nanometre scale and with a lag time of half a second. Circular DNA and human RAD54 protein were deposited in conditions favoring the partial attachment of DNA to mica in the presence of ATP. Displacements were analyzed as described above. Remarkably, the number of proteins that could be observed continuously interacting with DNA for several frames was low (about 10 of almost 500 analyzed). Only proteins that interacted with DNA during more than 5 frames (2.5 seconds) were considered in the analysis. High-speed AFM imaging enables the visualization of hopping-like events (fast translocations between DNA segments). Individual RAD54 molecules were observed to move from one dsDNA segment to another (Fig. 5, Movie 3, ESI†) here we call this hoping. The particle moved with a clear anomalous (not random) sub-diffusion ($\alpha = 0.24$) (Fig. 5c). The cumulative distribution plot shows that 40% of the hop lengths of that particle were of at least 10 nm ($P_{10} = 0.4$), resulting in faster movement on DNA than on the surface (see above) (Fig. 5d).

We also observed proteins tracking along DNA molecules by a process best described as one-dimensional diffusion (Fig. 6, Movie 4, ESI†). Displacements were possible to follow only for short periods of time (3 to 10 seconds). The limited amount of steps per trajectory measured required that we analyze the diffusion features of each sliding particle by calculating the probability distribution of square displacements.[51,57] The diffusion coefficient of a particle following a Brownian movement can be calculated after fitting the probability distribution with the exponential function:

$$P(x^2, \Delta t) = 1 - \exp\left(-\frac{x^2}{x_0^2(\Delta t)}\right)$$

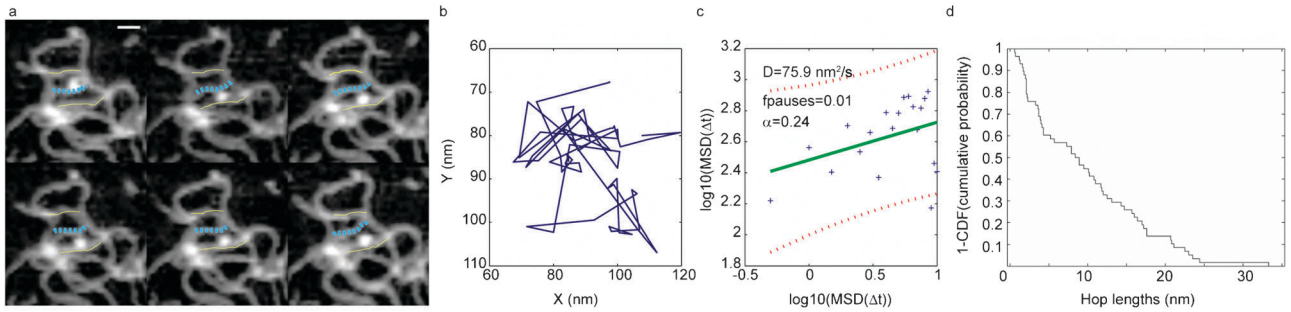

Fig. 5 Hopping on DNA as a cause of anomalous sub-diffusion. (a) Consecutive frames from Movie 3 (ESI†) (frames 2–7). Frames are separated by 500 ms, left to right continuing on subsequent lines. Movement of individual RAD54 molecules from one dsDNA segment (above the cyan line) to another (below the cyan line) without continuous contact was observed in a crowded environment, as a hopping-like mode (cropped images, original scan sizes 800 × 600 nm). Scale bar = 25 nm. (b) Scatter plot of x and y coordinates from the whole displacement. (c) Plot of the Log (MSD (Δt)) of the hopping protein *versus* log (Δt). Green lines = linear fit of the data. Red discontinuous lines = prediction bounds (95% confidence). The particle moved with a clear anomalous sub-diffusion ($\alpha = 0.24$). (d) The cumulative distribution of hop lengths (nm) normalized by the total number of hops ($n = 58$).

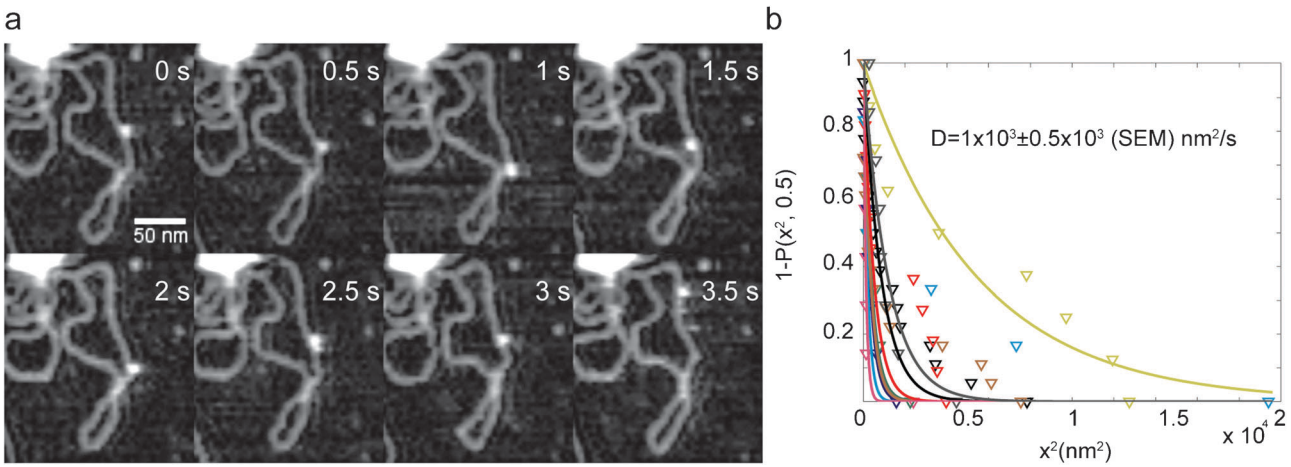

Fig. 6 RAD54 monomers slide on DNA in a diffusive Brownian manner. (a) Consecutive frames from Movie 4 (ESI†) (frames 1–8). Frames are separated by 500 ms, left to right continuing on subsequent lines. RAD54 monomer slides on a free segment of DNA. (b) Plot of the square displacement (x^2) *versus* $1 - P(x^2, \Delta t)$ of sliding proteins ($n = 9$).

where x^2 is the square displacement at Δt, and

$$x_0^2(\Delta t) = 2D\Delta t$$

Exponential fitting of the nine distributions measured showed variable goodness of fit from $r^2 = 0.73$ to $r^2 = 0.98$. The deviation from an exponential fit may reflect behavior that is not perfectly Brownian or a mixture of motions. Better goodness of fit was achieved by using a double exponential,[51] however the physical interpretation of this is not straightforward. Mono-exponential fitting shows that the diffusion of RAD54 was faster on DNA than on mica with diffusion coefficients ranging from 0.12×10^3 to 5.5×10^3 nm^2 s^{-1} (Fig. 6b). In the absence of nucleotide the diffusion coefficient on DNA was of the same order of magnitude. The fact that we did not observe sliding events for periods longer than a few seconds might be due to constraints in access to the DNA chain attached to the surface or to fast dissociation–association event. Although we cannot exclude the first possibility, we tested the second possibility by determining the effect of molecular crowding agents on bulk biochemical assays for RAD54 interaction with DNA. Specifically, DNA–RAD54 complexes formed in the absence of ATP were only detected in electrophoretic mobility shift assays if molecular crowding agents (BSA or PEG-6000) were included (Fig. S3, ESI†). This suggests fast dissociation/association could account for these observations.

Discussion

Here we describe the dynamic behavior of single human RAD54 proteins using high-speed AFM. Dynamic interaction of RAD54 with the sample surface was first characterized to define the experimental system and in order to distinguish this from specific biologically relevant interactions of RAD54 with DNA. Buffer composition and DNA had a notable effect on mobility of the protein on the surface. Brownian movement of RAD54 protein was decelerated six orders of magnitude by surface interaction, compared to diffusion in buffer, which in combination with high speed imaging (2 frames per second) permit the direct visualization of protein mobility. Increasing the concentration of ATP in the imaging buffer increased the protein diffusion constant. A similar effect was observed with a non-hydrolysable nucleotide analog (AMP-PNP) which ruled out an effect due to ATP hydrolysis. One reasonable explanation could be that nucleotide modified the surface charge. However salt concentrations mimicking the charge effect without the nucleotide resulted in the opposite effect. These might indicate a complex combination of electrostatic and hydrophobic interactions between the surface, the nucleotide and the protein that cannot be addressed solely by using this method. We have used cumulative probability distribution analysis[35,36,50–52] to show these subtle variations. In order to analyze individually the diffusion properties of RAD54 monomers, we estimated their diffusion coefficients after averaging the particle square displacements as a function of the time lag.[30,32,48,49] This method allows a straightforward discrimination between Brownian and anomalous diffusion.[30] Observation of protein movement by high-speed AFM revealed anomalous diffusion behavior that we could quantify in several situations.

Brownian diffusion occurs when interactions with surrounding molecules are negligible as is the case in most bulk biochemical reactions. However, the interior of a cell is far from this situation.[58] Using high-speed AFM we observed that the diffusion of RAD54 monomers tracking along DNA could be up to one order of magnitude faster than those moving on the surface. By using the full probability distribution of square displacements[51,57] it was possible to determine the sliding properties of RAD54.

Recently high-speed AFM imaging showed the hand-over-hand movement of Miosin V on an actin filament. Here we show that high-speed AFM is an appropriate technique for studying protein diffusion. Direct observation of biomolecules is possible without labeling, which may be impractical and often disturbs function. In addition because AFM imaging is based on the non-destructive interaction of a sharp tip and the sample, detection is not affected by chemical changes like photo-bleaching, blinking or oxidative by-products common in optically based methods. In general, AFM imaging conditions are fully compatible with biochemical reactions. The main limitation is the need for molecules to be attached to a surface for imaging. The choice of reactions to be studied has to take this into account. Potential disturbance of the observed sample by the scanning tip must also be considered,[59,60] which is however limited in tapping-mode high-speed AFM (<20 pN) and would not affect the sample significantly.[60]

RAD54 protein plays a role at many stages of the DNA repair by the homologous recombination process all of which required interaction with DNA, sometimes coupled to ATP hydrolysis and/or interaction with other proteins.[42,44] Using RAD54, several aspects of protein–DNA interactions could be detected and quantitatively described by high-speed AFM. Our experiments showed that monomer size RAD54 moved on DNA by diffusion. The presence or absence of ATP did not affect the sliding speed. We did observe directly that translocation of the protein in a DNA-crowded environment enhances the chance of hopping and facilitated transfer to different DNA locations. RAD54 is a dsDNA-dependent ATPase that can translocate along DNA.[45,46,61] A complete description of the structure and the activity of this molecular motor require tools with high spatial and temporal resolution. High-speed AFM is a valuable technique for the study of protein dynamics at the single molecule level. Particularly, DNA displacement by immobilized protein complexes can be analyzed with unprecedented spatial and temporal resolution. This will offer new ways of addressing highly dynamic processes of proteins interacting with and doing work on DNA.

Materials and methods

Proteins, reagents and sample preparation

The his6-tagged version of human RAD54 protein was expressed and purified in Sf21 insect cells as previously described.[46] Supercoiled pUC19 DNA was purified by CsCl density gradient centrifugation.

All chemicals used were of reagent grade. ATP was dissolved as concentrated stock solutions at pH 7.5. ATP concentrations were measured spectrophotometrically using

an extinction coefficient of 1.54×10^{-4} M^{-1} cm^{-1} at 260 nm and using the firefly luciferin-luciferase method.[62]

Protein–DNA binding reactions included 25 nM of purified RAD54 and 20 ng of supercoiled plasmid pUC19 in 10 mM HEPES–KOH, pH 7.5 and 2 mM $MgCl_2$. After incubation for 10 minutes at 30 °C, 3 microlitres of the binding reaction were deposited onto mica (1 mm^2) for 30 seconds. Surface was then rinsed with reaction buffer, with the indicated concentrations of nucleotide and $MgCl_2$, and the sample on mica was mounted over the cantilever of the microscope for observation. Temperature of the imaging buffer on the mica was 30 °C as measured with a probe.

Human RAD54 ATPase activity

The DNA-dependent RAD54 ATPase activity was assayed by thin-layer chromatography as described previously.[63] RAD54 (50 nM) and supercoiled dsDNA (5 nM of bp) were incubated with increasing concentrations of ATP (Fig. S4a, ESI†). The kinetics parameters in the first 5 minutes at 30 °C were K_m = 5.6 mM; K_{cat} = 6900 mol ATP min^{-1} mol $RAD54^{-1}$, r^2 = 0.99 from fitting to the Michaelis–Menten equation (Fig. 4a, ESI†). We tested the thermal stability of human RAD54 (Fig. 4b, ESI†) in the presence of 5 mM ATP and supercoiled dsDNA (5 nM of bp). At 30 °C the protein shows an exponential decay in activity with a half-life of 24.4 min. The catalytic constant at 20 °C was more stable with a half-life of 73 min. Therefore during AFM imaging (max 20 min) the protein maintains substantial activity comparable to the activity at room temperature.

High-speed atomic force imaging

The high-speed AFM imaging was performed in fluid with an NVB500 high-speed atomic force microscope (Olympus, Japan), operating in tapping mode[19] and using silicon nitride cantilevers (BL-AC7EGS-A2 cantilevers, Olympus, Japan). Each cantilever had a sharp probe tip deposited by electron beam deposition. The cantilevers had a 600–1000 kHz resonant frequency in water and 0.1–0.2 N m^{-1} spring constants.

Analysis of single molecule displacements

Distribution of protein displacement, or hop lengths, was analyzed by computing the empirical cumulative distribution function (CDF, "Statistic Toolbox" MATLAB). Probability of $1/n$ is assigned to each of n observations and then plotted as $y = 1 - \mathrm{CDF}$. $F(x)$ represents the proportion of observations in the sample more than or equal to x (nm). Raw data from image series generated by the microscope acquisition software (Olympus Corporation) were flattened and exported as avi files. Movies were contrast enhanced using ImageJ (available at http://rsb.info.nih.gov/ij; developed by Wayne Rasband, National Institutes of Health, Bethesda, MD). If necessary, to account for microscope drift, frames in the movies were aligned using StackReg plug-in for ImageJ.[64] Single molecule displacements were determined by measuring the distance travelled between two consecutive frames using MTrackJ plug-in (available at http://www.imagescience.org/meijering/software/mtrackj; developed by E. Meijering, Biomedical Imaging Group, Erasmus MC). The text file generated contained x and y positions of each particle per frame and the travelled distance between two consecutive frames. This information was used for calculating the deviation from Brownian movement, the mobility and the movement length (as defined in the Results section) for each particle. The MATLAB script used for the analysis is included as ESI† (supplementary software) as well as an example data sheet. The routine first calculates the mean square distance for each particle as described in ref. 32 using the average over all pairs.

Conclusions

The purpose of this work was to visualize the dynamics of the RAD54–DNA complex using a methodology that allows high spatial and sub-second temporal resolution. This study reveals that:

1. High-speed AFM is an appropriate technique for studying diffusion of proteins confined to a surface. The measured diffusion coefficient is six orders of magnitude lower than in solution.
2. Analysis of individual protein trajectories produces information usually hidden in ensemble averages.
3. The presence of nucleotide in the imaging buffer alters the motion of RAD54 protein on the surface, increasing the step size (Fig. 1) and favouring non-Brownian behaviour (Fig. 3).
4. Protein diffusion is confined by DNA corrals as directly visualized by high-speed AFM (Fig. 4).
5. Short range events representing different interactions modes of proteins with DNA ("hops" and "slides") were detectable and distinguishable by high-speed AFM (Fig. 5 and 6).

Acknowledgements

This work was supported by a Marie Curie grant from the European Commission (to H.S.), a VICI and a TOP grant from the Netherlands Organization for Scientific Research (NWO) (to C.W. and Roland Kanaar) and grants from the Japanese Ministry of Education, Culture, Sports, Science and Technology (Grant-in-Aid for Scientific Research on Priority Areas to K.T., for Young Scientists (B) to M. Y.) and from Japan Society for the Promotion of Science (Grant-in-Aid for Basic Research (A) to K.T.), and by SENTAN, JST (Japan Science and Technology Agency). Y.S. is a recipient of the JSPS (Japan Society for the Promotion of Science) research fellow. We thank to the Rene-Vogels Foundation for the support.

Notes and references

1 A. D. Riggs, S. Bourgeois and M. Cohn, *J. Mol. Biol.*, 1970, **53**, 401–417.
2 R. B. Winter, O. G. Berg and P. H. von Hippel, *Biochemistry*, 1981, **20**, 6961–6977.
3 T. Ruusala and D. M. Crothers, *Proc. Natl. Acad. Sci. U. S. A.*, 1992, **89**, 4903–4907.
4 A. Tafvizi, F. Huang, J. S. Leith, A. R. Fersht, L. A. Mirny and A. M. van Oijen, *Biophys. J.*, 2008, **95**, L01L–03.
5 P. C. Blainey, G. Luo, S. C. Kou, W. F. Mangel, G. L. Verdine, B. Bagchi and X. S. Xie, *Nat. Struct. Mol. Biol.*, 2009, **16**, 1224–1229.

6 J. Gorman, A. Chowdhury, J. A. Surtees, J. Shimada, D. R. Reichman, E. Alani and E. C. Greene, *Mol. Cell*, 2007, **28**, 359–370.
7 J. Gorman and E. C. Greene, *Nat. Struct. Mol. Biol.*, 2008, **15**, 768–774.
8 O. G. Berg, R. B. Winter and P. H. von Hippel, *Biochemistry*, 1981, **20**, 6929–6948.
9 K. Henzler-Wildman and D. Kern, *Nature*, 2007, **450**, 964–972.
10 S. E. Halford, *Biochem. Soc. Trans.*, 2009, **37**, 343–348.
11 D. R. Larson, *Nat. Methods*, **7**, 357–359.
12 A. Yildiz, J. N. Forkey, S. A. McKinney, T. Ha, Y. E. Goldman and P. R. Selvin, *Science*, 2003, **300**, 2061–2065.
13 G. Komazin-Meredith, R. Mirchev, D. E. Golan, A. M. van Oijen and D. M. Coen, *Proc. Natl. Acad. Sci. U. S. A.*, 2008, **105**, 10721–10726.
14 E. van der Linden, H. Sanchez, E. Kinoshita, R. Kanaar and C. Wyman, *Nucleic Acids Res.*, 2009, **37**, 1580–1588.
15 H. Sanchez, P. P. Cardenas, S. H. Yoshimura, K. Takeyasu and J. C. Alonso, *Nucleic Acids Res.*, 2008, **36**, 110–120.
16 A. Janicijevic, D. Ristic and C. Wyman, *J. Microsc.*, 2003, **212**, 264–272.
17 R. T. Dame, C. Wyman and N. Goosen, *J. Microsc.*, 2003, **212**, 244–253.
18 C. Bustamante, C. Rivetti and D. J. Keller, *Curr. Opin. Struct. Biol.*, 1997, **7**, 709–716.
19 M. Yokokawa, C. Wada, T. Ando, N. Sakai, A. Yagi, S. H. Yoshimura and K. Takeyasu, *EMBO J.*, 2006, **25**, 4567–4576.
20 F. Moreno-Herrero, M. de Jager, N. H. Dekker, R. Kanaar, C. Wyman and C. Dekker, *Nature*, 2005, **437**, 440–443.
21 D. J. Muller, A. Engel, U. Matthey, T. Meier, P. Dimroth and K. Suda, *J. Mol. Biol.*, 2003, **327**, 925–930.
22 M. Guthold, X. Zhu, C. Rivetti, G. Yang, N. H. Thomson, S. Kasas, H. G. Hansma, B. Smith, P. K. Hansma and C. Bustamante, *Biophys. J.*, 1999, **77**, 2284–2294.
23 T. Ando, N. Kodera, E. Takai, D. Maruyama, K. Saito and A. Toda, *Proc. Natl. Acad. Sci. U. S. A.*, 2001, **98**, 12468–12472.
24 P. K. Hansma, G. Schitter, G. E. Fantner and C. Prater, *Science*, 2006, **314**, 601–602.
25 N. Kodera, D. Yamamoto, R. Ishikawa and T. Ando, *Nature*, **468**, 72–76.
26 M. Yokokawa, S. H. Yoshimura, Y. Naito, T. Ando, A. Yagi, N. Sakai and K. Takeyasu, *IEE Proc.: Nanobiotechnol.*, 2006, **153**, 60–66.
27 J. L. Gilmore, Y. Suzuki, G. Tamulaitis, V. Siksnys, K. Takeyasu and Y. L. Lyubchenko, *Biochemistry*, 2009, **48**, 10492–10498.
28 N. Crampton, M. Yokokawa, D. T. Dryden, J. M. Edwardson, D. N. Rao, K. Takeyasu, S. H. Yoshimura and R. M. Henderson, *Proc. Natl. Acad. Sci. U. S. A.*, 2007, **104**, 12755–12760.
29 Y. Suzuki, Y. Higuchi, K. Hizume, M. Yokokawa, S. H. Yoshimura, K. Yoshikawa and K. Takeyasu, *Ultramicroscopy*, 2010, **110**, 682–688.
30 M. J. Saxton and K. Jacobson, *Annu. Rev. Biophys. Biomol. Struct.*, 1997, **26**, 373–399.
31 H. Qian, M. P. Sheetz and E. L. Elson, *Biophys. J.*, 1991, **60**, 910–921.
32 M. J. Saxton, *Biophys. J.*, 1997, **72**, 1744–1753.
33 D. M. Owen, D. Williamson, C. Rentero and K. Gaus, *Traffic (Copenhagen, Denmark)*, 2009, **10**, 962–971.
34 S. Wieser and G. J. Schutz, *Methods*, 2008, **46**, 131–140.
35 P. H. Lommerse, G. A. Blab, L. Cognet, G. S. Harms, B. E. Snaar-Jagalska, H. P. Spaink and T. Schmidt, *Biophys. J.*, 2004, **86**, 609–616.
36 S. M. van den Wildenberg, Y. J. Bollen and E. J. Peterman, *Biopolymers*, **95**, 312–321.
37 T. Kues, R. Peters and U. Kubitscheck, *Biophys. J.*, 2001, **80**, 2954–2967.
38 C. P. Bacher, M. Reichenzeller, C. Athale, H. Herrmann and R. Eils, *BMC Cell Biol.*, 2004, **5**, 45.
39 H. P. Babcock, C. Chen and X. Zhuang, *Biophys. J.*, 2004, **87**, 2749–2758.
40 E. Rothenberg, L. A. Sepulveda, S. O. Skinner, L. Zeng, P. R. Selvin and I. Golding, *Biophys. J.*, **100**, 2875–2882.
41 H. Ewers, A. E. Smith, I. F. Sbalzarini, H. Lilie, P. Koumoutsakos and A. Helenius, *Proc. Natl. Acad. Sci. U. S. A.*, 2005, **102**, 15110–15115.
42 W. D. Heyer, X. Li, M. Rolfsmeier and X. P. Zhang, *Nucleic Acids Res.*, 2006, **34**, 4115–4125.
43 A. V. Mazin, O. M. Mazina, D. V. Bugreev and M. J. Rossi, *DNA Repair*, **9**, 286–302.
44 T. L. Tan, R. Kanaar and C. Wyman, *DNA Repair*, 2003, **2**, 787–794.
45 T. L. Tan, J. Essers, E. Citterio, S. M. Swagemakers, J. de Wit, F. E. Benson, J. H. Hoeijmakers and R. Kanaar, *Curr. Biol.*, 1999, **9**, 325–328.
46 S. M. Swagemakers, J. Essers, J. de Wit, J. H. Hoeijmakers and R. Kanaar, *J. Biol. Chem.*, 1998, **273**, 28292–28297.
47 D. Ristic, C. Wyman, C. Paulusma and R. Kanaar, *Proc. Natl. Acad. Sci. U. S. A.*, 2001, **98**, 8454–8460.
48 G. J. Schutz, G. Kada, V. P. Pastushenko and H. Schindler, *EMBO J.*, 2000, **19**, 892–901.
49 S. Wieser, M. Moertelmaier, E. Fuertbauer, H. Stockinger and G. J. Schutz, *Biophys. J.*, 2007, **92**, 3719–3728.
50 M. Vrljic, S. Y. Nishimura, S. Brasselet, W. E. Moerner and H. M. McConnell, *Biophys. J.*, 2002, **83**, 2681–2692.
51 G. J. Schutz, H. Schindler and T. Schmidt, *Biophys. J.*, 1997, **73**, 1073–1080.
52 C. Loverdo, O. Benichou, R. Voituriez, A. Biebricher, I. Bonnet and P. Desbiolles, *Phys. Rev. Lett.*, 2009, **102**, 188101.
53 A. C. Storer and A. Cornish-Bowden, *Biochem. J.*, 1976, **159**, 1–5.
54 D. S. Banks and C. Fradin, *Biophys. J.*, 2005, **89**, 2960–2971.
55 J. A. Dix and A. S. Verkman, *Annu. Rev. Biophys.*, 2008, **37**, 247–263.
56 G. Guigas and M. Weiss, *Biophys. J.*, 2008, **94**, 90–94.
57 A. Sonnleitner, G. J. Schutz and T. Schmidt, *Biophys. J.*, 1999, **77**, 2638–2642.
58 D. S. Goodsell, *The machinery of life*, Copernicus Books, New York, N.Y., 2009.
59 T. van der Heijden, F. Moreno-Herrero, R. Kanaar, C. Wyman and C. Dekker, *Nano Lett.*, 2006, **6**, 3000–3002.
60 T. Ando, T. Uchihashi and T. Fukuma, *Prog. Surf. Sci.*, 2008, **83**, 337–437.
61 I. Amitani, R. J. Baskin and S. C. Kowalczykowski, *Mol. Cell*, 2006, **23**, 143–148.
62 G. E. Lyman and J. P. DeVincenzo, *Anal. Biochem.*, 1967, **21**, 435–443.
63 H. Sanchez and J. C. Alonso, *Nucleic Acids Res.*, 2005, **33**, 2343–2350.
64 P. Thevenaz, U. E. Ruttimann and M. Unser, *IEEE Trans. Image Process.*, 1998, **7**, 27–41.